Functional morphology and adhesive performance of the stick-capture apparatus of the rove beetles *Stenus* spp. (Coleoptera, Staphylinidae)

Lars Koerner[a,*], Stanislav N. Gorb[b], Oliver Betz[a]

[a] *Department of Evolutionary Biology of Invertebrates, Institute for Evolution and Ecology, University of Tübingen, Auf der Morgenstelle 28E, D-72076 Tübingen, Germany*
[b] *Department of Functional Morphology and Biomechanics, Zoological Institute, University of Kiel, Am Botanischen Garten 1-9, D-24098 Kiel, Germany*

ARTICLE INFO

ABSTRACT

The adhesive prey-capture apparatus of the representatives of the rove beetle genus *Stenus* (Coleoptera, Staphylinidae) is an outstanding example of biological adhesive systems. This unique prey-capture device is used for catching elusive prey by combining (i) hierarchically structured adhesive outgrowths, (ii) an adhesive secretion, and (iii) a network of cuticular fibres within the pad. The outgrowths arise from a pad-like cuticle and are completely immersed within the secretion. To date, the forces generated during the predatory strike of these beetles have only been estimated theoretically. In the present study, we used force transducers to measure both the compressive and adhesive forces during the predatory strike of two *Stenus* species. The experiments revealed that the compressive forces are low, ranging from 0.10 mN (*Stenus bimaculatus*) to 0.18 mN (*Stenus juno*), whereas the corresponding adhesive forces attain up to 1.0 mN in *S. juno* and 1.08 mN in *S. bimaculatus*. The tenacity or adhesive strength (adhesive force per apparent unit area) amounts to 51.9 kPa (*S. bimaculatus*) and 69.7 kPa (*S. juno*). *S. juno* beetles possess significantly smaller pad surface areas than *S. bimaculatus* but seem to compensate for this disadvantage by generating higher compressive forces. Consequently, *S. juno* beetles reach almost identical adhesive properties and an equal prey-capture success in attacks on larger prey. The possible functions of the various parts of the adhesive system during the adhesive prey-capture process are discussed in detail.

© 2012 Elsevier GmbH. All rights reserved.

1. Introduction

So far, most studies on animal adhesive organs have focused on the adhesive pads of legs in the context of locomotion. Adhesive structures of mouthparts used in prey capture have been less extensively studied (reviewed in Betz and Kölsch, 2004). An outstanding adhesive prey-capture apparatus is formed by the labium of rove beetles of the genus *Stenus* Latreille, 1797 (e.g., Weinreich, 1968) (Fig. 1). This system belongs to the hairy, branched and wet (with adhesive fluid) type.

The genus *Stenus* comprises more than 2500 species worldwide and is therefore one of the most diverse beetle genera (Puthz, 2010). Their elongated labium can be protruded towards the potential prey extremely rapidly (within 1–3 ms) by haemolymph pressure (Bauer and Pfeiffer, 1991). The paraglossae at the distal end of the rod-like prementum are modified into sticky pads (Figs. 1 and 2A), whose surface is differentiated into terminally branched outgrowths (Fig. 2B). As soon as the prey adheres to these sticky pads, the labium is instantly retracted and the beetle can seize the prey with its mandibles. The structure and function of this

adhesion-capture apparatus have been described in several previous publications (e.g., Schmitz, 1943; Weinreich, 1968; Betz, 1996, 1998; Kölsch and Betz, 1998; Kölsch, 2000; Betz et al., 2009). Most *Stenus* species make use of their mandibles as an alternative prey-capture technique (Bauer and Pfeiffer, 1991; Betz, 1996, 1998).

The sticky pads maintain their adhesive function via an adhesive secretion that is produced in specialised glands within the head capsule (Schmitz, 1943; Weinreich, 1968) and secreted onto the pad surface (Fig. 2C and D). The secretion has been assumed to consist of at least two immiscible phases: proteinaceous and lipoid (Kölsch, 2000). The biphasic nature of the secretion might be advantageous for effective spreading over substrates with various surface energies.

The prey-capture apparatus of *Stenus* spp. functions like a catapult (see supplementary video mmc1 in Appendix A), i.e., the elastic elements of the labium are preloaded indirectly via increased haemolymph pressure prior to the strike and are finally released to hit the prey suddenly with high impact pressure (Kölsch and Betz, 1998; Betz, 1998, 1999, 2006). The antagonists of this system are represented by large retractor muscles of the mouth angles (Weinreich, 1968). When the labium is retracted, adhesive forces develop perpendicularly with respect to the prey surface (Betz, 2006). In contrast to tarsal attachment devices, in which van der Waals and capillary forces are considered to be the major
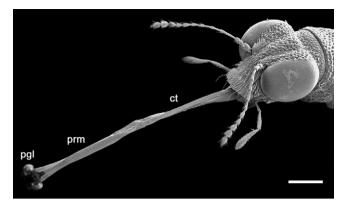
Fig. 1. The adhesion-capture apparatus of *Stenus bimaculatus*. Scanning electron microscopic image of the head with the protruded labium. Scale bar = 0.5 mm. Abbreviations: ct = connecting tube, pgl = paraglossa, prm = prementum.

adhesive mechanisms (e.g., Stork, 1980; Alexander, 1992; Autumn et al., 2002; Langer et al., 2004; Huber et al., 2005), viscous forces (Stefan adhesion) are assumed to be the major adhesive mechanism of the *Stenus* labium (Kölsch, 2000; Betz and Kölsch, 2004). According to Betz (1996), the sticky pads of the labium have been modified in various ways from a general type during the course of evolution. These changes mainly involve (i) the area of the sticky pads, (ii) the number of outgrowths on the pads, and (iii) the degree of branching of single outgrowths. These morphological parameters greatly influence prey-capture success, which is presumably based on differences in the adhesive performance (Betz, 1996, 1998).

To date, the attractive forces that act during the predatory strike of the *Stenus* labium have only been indirectly estimated (Kölsch, 2000). According to these calculations, the strongest expected viscosity-based adhesive force in the species *Stenus comma* LeConte

amounts to 66.4 μN. However, direct measurements of adhesive forces are lacking in the literature. The present study presents *in vivo* force measurements carried out during the predatory strike of two species of the genus *Stenus*.

The following questions have been addressed in our study. (i) What functional principles underlie the adhesive prey-capturing mechanism of *Stenus*? (ii) How does the morphology of the labial adhesive pads influence adhesion? (iii) Is there a correlation between the generated compressive (impact) force and the adhesive force? The forces measured in the present study are compared with forces previously obtained from other adhesive systems of insects, such as tarsal attachment devices.

2. Materials and methods

2.1. Animals

Studies were carried out with adult *Stenus juno* Paykull 1800 and *Stenus bimaculatus* Gyllenhal 1810. Both these species were collected from the reed zone of a small pond near Tuebingen, southern Germany (48°31′30.74″N, 9°00′46.53″E). They were kept in the laboratory in plastic boxes lined with moist gypsum plaster mixed with activated charcoal to prevent contamination with microorganisms and to ensure a constant high humidity. Beetles were fed with living collembolans ad libitum.

2.2. Force measurements on living beetles

Before the experiments were performed, the beetles were starved for 5–7 days. The experimental set-up for determining the compressive and adhesive forces generated during the beetles' predatory strike is shown in Fig. 3. The spherical head of an insect pin (No. 00; Morpho, Austria) with a diameter of 1.0 mm was used as a dummy prey. It was connected to a force sensor (FORT25; WPI
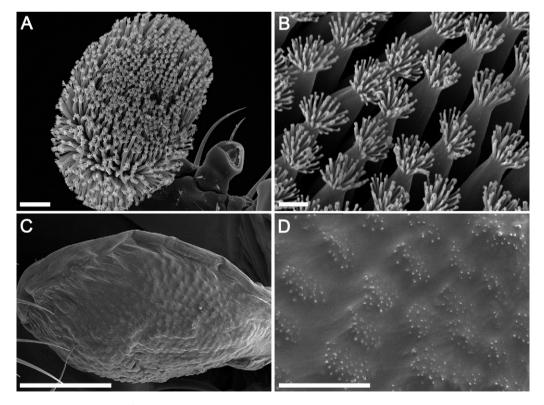

Fig. 2. Images of the paraglossae, which are modified into sticky pads, in *Stenus juno*. (A–B) SEM images, (C–D) cryo-SEM images. (A) Ventral aspect of a sticky pad. Scale bar = 20 μm. (B) Adhesive outgrowths with terminal ramifications. Scale bar = 2 μm. (C) During prey capture, the adhesive outgrowths are deeply immersed within the adhesive secretion. Scale bar = 30 μm. (D) Adhesive secretion with protruding terminal ramifications of the adhesive outgrowths. Scale bar = 2 μm.
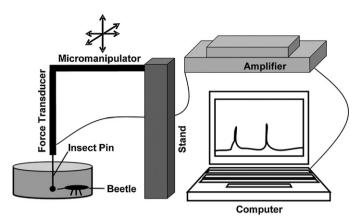
Fig. 3. Experimental set-up for force measurements during dummy prey-capture. The beetle is located in a circular arena. The head of an insect pin is used as dummy prey. The pin is fixed to a force transducer that is connected to a micromanipulator, which is movable in various directions to attract the attention of the beetle. When the beetle strikes the insect pin, the resulting forces are amplified and recorded.

Inc., Sarasota, FL, USA) that was calibrated prior to the experiments by means of a 20 mN weight. Since the adhesive and compressive forces generated during the predatory strike develop perpendicular to the surface, we used a single-axis force sensor for our measurements. Because the beetles only react to moving objects, the force sensor with the attached insect pin was mounted on a micromanipulator that was moved back and forth to attract the beetles' attention. The force sensor was attached to an amplifier (BIOPAC Systems Inc., Goleta, CA, USA) and a computer-based data-acquisition and processing system (MP100 WSW, BIOPAC Systems Inc., USA). The strike of the beetle at the dummy caused force sensor deflection that was digitally recorded and later processed. After each individual test, the insect pin was cleaned with ethanol (70%) and distilled water. The experiments were performed with 27 individuals of each species, with 15–25 strikes per individual beetle. The maximum compressive and adhesive forces of each beetle were obtained by means of the software AcqKnowledge 3.8.2 (BIOPAC Systems Inc., USA) and used for statistical evaluation. Prior to the experiments, the beetles were weighed individually by using an analytical balance (GR-202-EC Dual Range; A&D Instruments Ltd., Abingdon, UK).

The free surface energy of the insect pin and its dispersive and polar components were measured by using a video-based optical contact angle-measuring device (OCAH 200; Dataphysics Instruments GmbH, Filderstadt, Germany). The free surface energy was calculated by using a series of liquids (water, diiodomethane, ethylene glycol). The contact angles of the liquids on the insect pin were evaluated by the sessile drop method (droplet volume: 1 μl) and ellipse-fitting. The surface energy and its components were determined according to the Owens–Wendt–Kaelble method (Owens and Wendt, 1969). The contact angle of water of the head of the insect pin was $84.03 \pm 1.7°$ ($n = 4$) and its surface energy was 30.77 ± 1.4 mN/m (dispersive component: 26.9 ± 1.3 mN/m; polar component 3.8 ± 0.4 mN/m).

2.3. High-speed video recordings

Representative predatory strikes on the insect pin were recorded at 2000 frames s^{-1} with a high-speed camera (Kodak Motion Corder Analyzer PS-110; Eastman Kodak Company, Rochester, NY, USA) mounted on a binocular microscope (Leica MZ6; Leica Microsystems, Wetzlar, Germany).

2.4. Microscopy techniques

For scanning electron microscopy (SEM), beetle heads with the labia extended were cleaned with H_2O_2, dehydrated in an ethanol series, critical-point dried (Polaron E3000; Quorum Technologies, East Grinstead, UK), fixed to stubs with silver paint, sputter-coated with gold–palladium (SCD 030; Balzers Instruments, Balzers, Liechtenstein) and observed in a stereoscan 250 MK2 SEM (Cambridge Instruments, Cambridge, UK). The following morphological parameters of the sticky pads were measured with tpsDig 1.40 (Rohlf, 2004): (1) surface area of the sticky pads, (2) number of adhesive outgrowths per sticky pad, (3) length, (4) diameter and (5) cross-sectional area of the shaft of a single outgrowth, (6) number of terminal ramifications per adhesive outgrowth and (7) length, (8) diameter and (9) cross-sectional area of a single ramification. The length, diameter, and cross-sectional area (calculated from the diameter) of the outgrowths and ramifications as well as the number of ramifications were measured at the centre of the sticky pad (for a given specimen, the mean of five measurements of each variable was calculated). The aspect ratios of the outgrowths and ramifications were calculated by dividing their lengths by their diameters. The newly obtained data of the surface area of the sticky pads, the number of adhesive outgrowths per sticky pad, the number of terminal ramifications per adhesive outgrowth and the number of terminal ramifications per sticky pad were merged with the data obtained by Betz (1996).

For cryo-SEM, the heads with the extended labia were glued to holders with Tissue-Tek OCT compound (Sakura Finetek Europe B.V., Zoeterwoude, The Netherlands) or were mechanically gripped in a small vice on holders. The specimens were frozen in liquid nitrogen and transferred to a cryo-stage of the preparation chamber at $-140°C$ (Gatan ALTO 2500 cryo-preparation system; Gatan Inc., Abingdon, UK). Frozen samples were sublimated at a temperature of $-90°C$ for 3 min, sputter-coated with gold–palladium (thickness 6 nm) and studied in a cryo-SEM Hitachi S-4800 (Hitachi Corp., Tokyo, Japan) at an accelerating voltage of 3 kV and $-120°C$. This allowed us, for the first time, to visualise labium structures with the adhesive secretion located on their surfaces at high resolution.

To visualise secretion prints left on the dummy prey, the head of the insect pin was coated with gold–palladium and examined by conventional SEM (Cambridge Stereoscan 250 MK2; Cambridge Instruments, Cambridge, UK) as described above.

Additionally, the thickness profile of the cured secretion prints left on the surface of clean cover glasses (Nr. 0; Hecht, Sondheim, Germany) was analysed by using a scanning white light interferometer (Zygo NewView 5000; Zygo Corp., Middlefield, CT, USA).

2.5. Bright-field light microscopy and fluorescent microscopy

To visualise resilin-bearing parts of the prey-capture apparatus, the labia of freshly killed beetles were cut off, mounted on cover-slips in a water-soluble medium (Moviol; Hoechst, Frankfurt, Germany) and observed by fluorescence microscopy (Zeiss Axioplan; Carl Zeiss Inc., Oberkochen, Germany) under bright-field illumination or one of three wavelength bands: green (excitation 512–546 nm, emission 600–640 nm), red (excitation 710–775 nm, emission 810–890 nm) or ultraviolet (excitation 340–380 nm, emission 425 nm). Images taken in the fluorescence mode were superimposed in order to show the autofluorescence of the cuticular structures (Gorb, 1999, 2004; Niederegger and Gorb, 2003; Perez Goodwyn et al., 2006). Insect cuticle has strong autofluorescence at wavelengths from blue-green to deep-red, whereas resilin has autofluorescence at a narrow band of wavelengths around 400 nm (Andersen and Weis-Fogh, 1964) and therefore appears blue in fluorescence images.
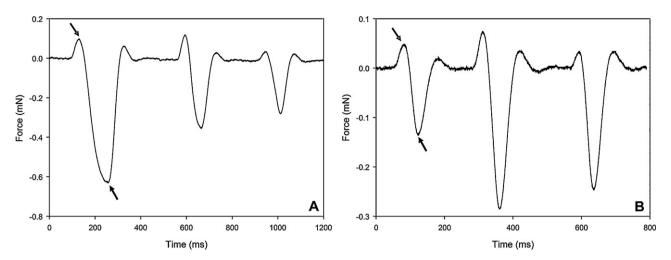
Fig. 4. Representative force–time curves of three consecutive strikes of (A) *S. juno* and (B) *S. bimaculatus* on the dummy prey. Upon prey capture, the labium transfers a definite impact force (compressive force) to the dummy prey, as indicated by the first arrows. The second arrows indicate the maximum adhesive force that arises during the retraction of the labium. Note that the compressive forces are much lower than the resulting adhesive forces.

2.6. Prey-capture experiments

To obtain a higher sample size, additional prey-capture experiments were conducted on *Heteromurus nitidus* Templeton 1835 springtails of various sizes according to Betz (1996, 1998). Similar to his experiments, 10–15 attacks per specimen were evaluated. The newly obtained data were added to the data of *S. bimaculatus* and *S. juno* obtained by Betz (1996, 1998) and statistically analysed. The fresh weights ranged from 8.4 ± 5.6 μg in "small" springtails to 62.3 ± 25 μg in "large" springtails (data from Betz, 1996, 1998).

2.7. Statistical analyses

Statistical analyses were performed with SPSS 11.0 (SPSS Inc., Chicago, IL, USA). Data were tested for normality by using the Shapiro–Wilk test. If the data followed the normal distribution, Student's *t*-test was used for further analysis. Otherwise, the Mann–Whitney *U*-test was employed.

3. Results

3.1. Force measurements

Both the impact (compressive) forces of the labium hitting the dummy prey and the resulting adhesive forces were directly measured in the investigated *Stenus* beetles. Examples of typical force–time curves are shown in Fig. 4A and B. Upon prey-capture strike, the labium transmits a compressive force F_c to the prey. The mean compressive forces amounted to 0.102 mN for *S. bimaculatus* and 0.179 mN for *S. juno* (Table 1, Fig. 5). These differences were significant (t-test, $t = -5.90$, df = 52, $p < 0.001$). During the retraction of the sticky pads from the contacted surface, an adhesive force F_a could be measured (Fig. 4). The average adhesive forces did not differ statistically between *S. bimaculatus* (1.1 mN, $N = 27$) and *S. juno* (1.0 mN, $N = 27$) (Table 1, Figs. 4 and 5; *t*-test, $t = 1.32$, 34 df = 52, $p > 0.05$).

Our measurements showed that in both species investigated the compressive force was significantly lower than the resulting adhesive force (Fig. 5; paired *t*-test, *S. bimaculatus*: $t = -22.44$, df = 26, $p < 0.001$; *S. juno*: $t = -22.48$, df = 26, $p < 0.001$). The maximum F_a/F_c ratio was significantly higher in *S. bimaculatus* (11.41 ± 3.6; $N = 27$) than in *S. juno* (6.21 ± 2.5; $N = 27$) (*t*-test, $t = 6.18$, df = 52, $p < 0.001$).

The mean tenacities (average adhesive forces divided by the mean surface areas of the sticky pads) amounted to 51.89 kPa in *S.*
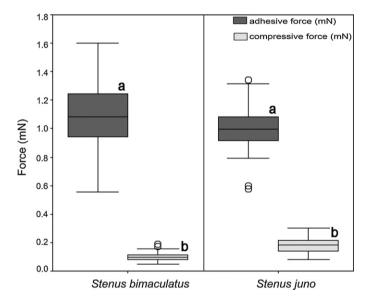

Fig. 5. Maximum adhesive (dark grey boxes) and compressive forces (light grey boxes) in *S. bimaculatus* and *S. juno*. Plot shows medians (centre lines), interquartile ranges (boxes), maximum and minimum values (whiskers), and outliers (circles). The outliers are cases with values between 1.5 and 3 box-lengths from the 75th percentile or 25th percentile. Different letters indicate statistical differences between the compressive and adhesive forces of each species (paired *t*-test). $n = 27$.

bimaculatus and 69.65 kPa in *S. juno* (Table 1). Within each species, no or only weak relationships seemed to be present between the compressive and the resulting adhesive force. In both species, both variables positively correlated in only 3 out of the 27 individuals tested.

3.2. Morphology of the sticky pads

The ventral part of each paraglossa is modified into a sticky pad that is covered with a large number of brush-like adhesive outgrowths that are terminally differentiated into numerous ramifications (Fig. 2A and B). Strong interspecific differences exist in the morphology of the sticky pads of *Stenus* beetles, especially with respect to their surface area, the number of adhesive outgrowths and the number of adhesive contacts (Betz, 1996).

The morphological characters of the sticky pads of the two investigated species are summarised in Table 2. The two species differ

Table 1
Body mass, compressive, and adhesive forces obtained during the predatory strike on the dummy prey by *S. bimaculatus* and *S. juno*. Values are presented as means ± standard deviations. Force/weight ratios are given in parentheses. $N = 27$. p = significance level of tests for differences of the means between both species (t-test).

	S. bimaculatus	p	S. juno
Body mass [mg]	5.052 ± 0.35	***	3.526 ± 0.37
Compressive force [mN]	0.102 ± 0.04 (2.07)	***	0.179 ± 0.06 (5.25)
Adhesive force [mN]	1.077 ± 0.24 (21.91)	n.s.	1.000 ± 0.19 (29.13)
Ratio adhesive/compressive force	11.408 ± 3.57	***	6.213 ± 2.53
Tenacity [kPa]	51.89	–	69.65

n.s., $p > 0.05$.
*** $p < 0.001$.

Table 2
Morphological parameters of the sticky pads in *S. bimaculatus* and *S. juno*. Values are presented as means ± standard deviations (SD). The number of individuals used (N) is indicated for all parameters. p = significance level of tests indicating differences of the means between both species (t-test).

Morphological parameter	S. bimaculatus				S. juno		
	N	Mean	SD	p	N	Mean	SD
Surface area of the sticky pad [μm^2]	20	10,755.13	1728.1	***	19	7176.94	1108.4
Adhesive outgrowths per sticky pad	14	586.21	51.0	n.s.	14	590.64	83.0
Adhesive outgrowths per μm^2	14	0.054	0.01	***	14	0.083	0.02
Length of outgrowth [μm]	9	24.98	2.4	***	6	20.30	0.8
Diameter of outgrowth [μm]	9	2.51	0.1	*	6	2.71	0.2
Cross-sectional area of shaft of outgrowth [μm^2]	9	4.99	0.3	*	6	5.84	0.8
Aspect ratio of outgrowth	9	10.03	0.9	***	6	7.57	0.6
Terminal ramifications per outgrowth	9	28.91	1.7	n.s.	8	25.23	6.8
Terminal ramifications per sticky pad	13	17,910.64	3030.4	n.s.	9	16401.15	3700.0
Terminal ramifications per surface area of 1 μm^2	13	1.64	0.3	***	9	2.34	0.5
Length of terminal ramification [μm]	9	1.62	0.1	*	6	1.45	0.1
Diameter of single terminal ramification [μm]	9	0.237	0.04	***	6	0.171	0.02
Cross-sectional area of terminal ramification [μm^2]	9	0.049	0.03	*	6	0.024	0.01
Aspect ratio of terminal ramification	9	7.16	0.7	*	6	8.63	1.4

n.s., $p > 0.05$.
* $p < 0.05$.
*** $p < 0.001$.

significantly in the area of their sticky pads (t-test; $t = -8.74$, df = 46, $p < 0.001$), whereas the number of adhesive outgrowths and adhesive contacts per sticky pad and the number of ramifications per adhesive outgrowth do not differ significantly. In relation to the shaft of the adhesive outgrowth, the terminal ramifications are extremely short (ratio shaft/terminal ramifications: *S. bimaculatus*, 15.38; *S. juno*, 13.96) and have a much smaller cross-sectional area (ratio cross-sectional area of the shaft/cross-sectional area of its terminal ramifications: *S. bimaculatus*, 101.84; *S. juno*, 243.33). Both investigated species possess outgrowths and ramifications with high aspect ratios. The average aspect ratio of the outgrowths for *S. bimaculatus* was 10.03 ($N = 9$) and for *S. juno* 7.57 ($N = 6$), whereas the aspect ratio of the ramifications for *S. bimaculatus* was 7.16 ($N = 9$) and for *S. juno* 8.63 ($N = 6$) (Table 2). The outgrowths are arranged at a right or slightly oblique angle ($\leq 90°$) relative to the surface of the sticky pad (Fig. 2A). In both species the tips of the ramifications are spherically shaped.

3.3. Adhesive secretion

During prey capture, the outgrowths are deeply immersed in the adhesive secretion (Fig. 2C), with only the tips of their terminal ramifications slightly protruding (Fig. 2D). Both the high-speed video recordings (Fig. 6; see also supplementary video no. 2 in Appendix A) and the secretion prints (Fig. 7) show that an exceptionally large amount of secretion is involved in the prey-capture process. Furthermore, these images suggest that the secretion is highly viscous (Figs. 6, frames 10–14 and 7B), since it stretches and splits into long fibres (fibrillation) before it finally tears off at the contact zone with the substratum. According to our high-speed video recordings (see supplementary video mmc2 in Appendix A), the sticky pads, while being retracted from the head of the insect pin, are stretched

longwise first (Fig. 6, frames 5–9; indicative of their low E-modulus), followed by the stretching of the secretion (Fig. 6, frames 9–14).

White-light interferometry revealed a minimum secretion layer thickness of the prints left on the glass surface of about 30–150 nm. The actual value might even be lower, since it was estimated from secretion prints after retraction of the sticky pads from the glass surface.

3.4. Resilin occurrence

Fluorescence microscopy revealed the presence of resilin in the material of the entire sticky pads; high concentrations of resilin are also present within the mobile joints (e.g., of the labial palpus) (Fig. 8C and D).

3.5. Prey-capture experiments

The prey-capture experiments revealed a higher prey-capture success in *S. juno* for small springtails (Table 3: Mann–Whitney *U*-test; $Z = -3.49$; $p < 0.001$), whereas no difference between the two species was detected for large springtails (Table 3). In both of these species, the prey-capture success in attacks on small springtails was significantly higher than that on large springtails (*S. bimaculatus*: Mann–Whitney *U*-test, $Z = -5.71$, $p < 0.001$; *S. juno*: Mann–Whitney *U*-test, $Z = -6.61$, $p < 0.001$).

3.6. Mechanism of adhesion

In order to determine the physical mechanism of adhesion involved in the prey capture of *Stenus* beetles we calculated the theoretical adhesive forces and compared them with the measured
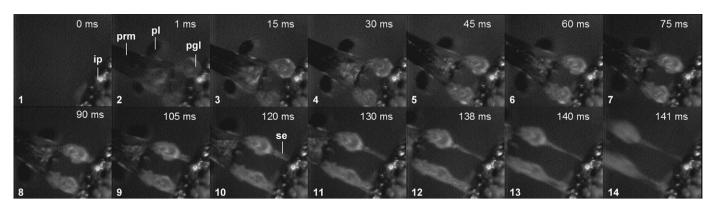
Fig. 6. High-speed video images of the strike on the head of an insect pin in *S. bimaculatus*. The insect pin is situated on the right side, whereas both sticky pads approach from the left. The actual strike lasts only 1 ms (frames 1–2). The time line of the depicted sequence is indicated in milliseconds in the upper right corner of each frame. The adhesive secretion is viscous, as can be seen in frames 9–14, in which it is stretched out into long fibres. The sticky pads are extremely flexible (frames 5–13) and stretch in length just before the secretion stretches. Scale bar = 50 μm. Abbreviations: ip = insect pin, pl = palpus labialis, pgl = paraglossa, prm = prementum, se = secretion.
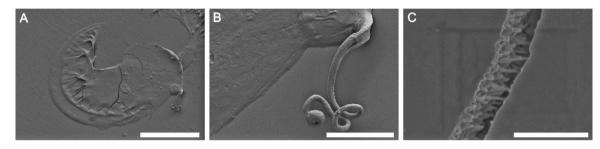

Fig. 7. SEM images of the secretion left on the dummy prey by *S. juno*. (A) Whole secretion print. Scale bar = 50 μm. (B) During retraction of the sticky pads, the secretion stretches into long fibres until it breaks. The depicted fibre is indicative of the high viscosity of the secretion. Scale bar = 10 μm. (C) Example of the fibrillar structures inside the secretion. Scale bar = 1 μm.
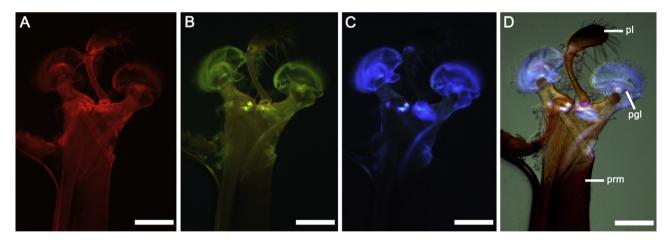

Fig. 8. Light micrographs of the labium of *S. bimaculatus*. View in (A) the green band (excitation 512–546 nm, emission 600–640 nm), (B) the red band (excitation 710–775 nm, emission 810–890 nm), and (C) the UV band (excitation 340–380 nm, emission 420 nm). (D) All three images taken at various wavelengths (A–C) superimposed. Resilin exhibits auto-fluorescence in an extremely narrow wavelength band (ca. 400 nm) so that it can only be seen in the UV band (C and D). Scale bars = 85 μm. Abbreviations: pl = palpus labialis, pgl = paraglossa, prm = prementum.

Table 3
Percentage of successful attacks conducted with the labium by *S. bimaculatus* and *S. juno* on small and large springtails (*Heteromurus nitidus*). Values are presented as means ± standard deviations. *p* = significance level of tests for differences between both species (Mann–Whitney *U*-test), *n* = number of individuals tested (according to Betz, 1996, 1998).

Successful attacks conducted with the labium [%]	*S. bimaculatus*	*p*	*S. juno*
Small springtails	64.72 ± 23.1 (*n* = 43)	***	81.87 ± 16.6 (*n* = 43)
Large springtails	28.36 ± 22.5 (*n* = 42)	n.s.	29.78 ± 27.9 (*n* = 39)

n.s., *p* > 0.05.
*** *p* < 0.001.

ones. The theoretically determined adhesive force attributable to Stefan adhesion was calculated with the formula (Bowden and Tabor, 1950; Kölsch, 2000):

$$F_{\text{Viscosity}} = \frac{3\pi\eta R^4}{4td^2} \tag{1}$$

and amounted to 0.98×10^{-3} N in *S. juno* and 2.21×10^{-3} N in *S. bimaculatus*. The following values were used for these calculations: (1) the radius (R) of the sticky pad (estimated from the pad area): 4.78×10^{-5} m (*S. juno*) and 5.85×10^{-5} m (*S. bimaculatus*), (2) the thickness of the secretion layer (d): 5×10^{-8} m as measured by white-light interferometry, (3) the time required for the separation of the surfaces to infinity (t): 0.1 s (Fig. 6), and (4) the viscosity of the adhesive (η): 0.01 N s m^{-2} (similar to that of vegetable oils; Kölsch, 2000).

The force of adhesion attributable to surface tension can be calculated as:

$$F_{\text{surface tension}} = 4\pi R\gamma \cos\theta, \tag{2}$$

where R is the radius of the sticky pad, γ is the surface tension of the fluid, and θ is the contact angle of the fluid (McFarlane and Tabor, 1950; Israelachvili, 1991; Kölsch, 2000). Apart from the radius of the sticky pads (see above), the following values were inserted into the calculation: (1) the surface tension of the secretion: 72 mJ m^2 (Kölsch, 2000) and (2) the contact angle of the fluid to the surface: 30° (estimated from white-light interferometry and SEM images). According to this calculation, the forces attributable to the surface tension of the secretion amounted to 7.49×10^{-5} N in *S. juno* and 9.17×10^{-5} N in *S. bimaculatus*.

4. Discussion

Complementing our study on the adhesive performance toward various surfaces (Koerner et al., 2012), the present study follows a more general approach, combining morphological analyses and force experiments in order to determine the forces that occur during the course of the prey-capture process in two species of the genus *Stenus*. These experiments helped to enhance our understanding of the underlying functional principles of this adhesive prey-capture mechanism (Fig. 9).

4.1. External morphology

The external structures of the labial sticky pads of *Stenus* beetles must have been subject to strong selective forces during their evolution (Betz, 1996). In *Stenus* species whose labial sticky pads have larger surface areas (e.g., *S. bimaculatus*, *S. juno*, *S. latifrons*), a higher number of adhesive outgrowths and adhesive contacts has experimentally been shown to lead to improved adhesion and thus to increased prey-capture success (Betz, 1996, 1998).

Adhesion between an adhesive pad and a substrate can be increased by splitting up the contact zone into many subcontacts, especially on uneven substrates (Varenberg et al., 2006, 2010). This principle can be seen in *Stenus* species, where the labial sticky pads show a hierarchical structure comprising the surface of the sticky pads with numerous adhesive outgrowths and their extremely fine terminal ramifications (Fig. 2; Table 2). The functional advantage of a hierarchically organised structure lies in the break-up of the adhesive surface into a large number of independent elements that compensate for possible surface irregularities of the prey (Betz and Kölsch, 2004). Contact splitting also ensures defect tolerance since the failure of a single element or a few elements does not impact the adhesion of the ensemble significantly (Spolenak et al., 2005b). In *Stenus* species, the subdivision of the contacts leads to enhanced adhesion, although in the present case of a "flooded

regime" (Bhushan, 2003; Mate, 2008), in which the adhesive contacts are deeply immersed within the secretion (cf. Fig. 2C and D), the actual number of single contacts should be less important than the perimeter of the entire sticky pad.

A spherically shaped contact provides good adhesion, if the radius of the contact is reduced to scales below 100 nm (Spolenak et al., 2005b). Therefore, the spherically shaped tips of the ramifications in *Stenus* species (cf. Fig. 2B), with radii from 80 to 120 nm (as approximated from the diameter), might not only result in intimate contact with small-scale surface irregularities, but also ensure adhesion, although a large amount of viscous secretion is still needed. Additionally, the high aspect ratio of both the outgrowths and the ramifications in *Stenus* species (Table 2) makes these structures more compliant and therefore improves their adaptability to the uneven profile of the prey surface, comparable to the tarsal adhesive setae of insects (Kölsch and Betz, 1998; Peressadko and Gorb, 2004; Chan et al., 2007; Voigt et al., 2008).

In tarsal adhesive pads, a branched morphology of the setae is additionally advantageous, because the condensation between neighbouring setae is reduced as a result of the stronger stiffness of same-level neighbouring branches as compared to the adhesive strength of contacting spatula (Jagota and Benninson, 2002; Spolenak et al., 2005a; Federle, 2006). *Stenus juno* beetles have a significantly higher density of adhesive outgrowths than *S. bimaculatus* beetles (Table 2), which makes such structures potentially more susceptible to condensation (Jagota and Benninson, 2002; Spolenak et al., 2005a; Federle, 2006). However, *S. juno* beetles seem to have evolved various morphological adaptations to avoid this problem. First, these beetles have shorter, but wider and thus presumably stiffer, adhesive outgrowths than *S. bimaculatus*. Additionally, *S. juno* beetles possess an equally large number of shorter and more densely packed ramifications (Table 2). Embedding of the outgrowths within the adhesive secretion in both species (Fig. 2D) provides further protection against condensation because of the absence of capillarity and reduced van der Waals interactions (Israelachvili, 1991).

4.2. Adhesive performance

Our *in vivo* force measurements revealed much lower values for the compressive force than for the resulting adhesive force (Table 1). Thus, in *Stenus* beetles the ratio of the adhesive force and the applied (compressive) force is much higher (6.21 in *S. juno* and 11.41 in *S. bimaculatus*) than in tarsal adhesive systems (Table 1, Fig. 5); e.g., in the cricket *Tettigonia viridissima* L. (Ensifera, Tettigoniidae), the value of this ratio lies between 1.6 and 3.5 (as calculated from Fig. 6B in Jiao et al., 2000). Accordingly, the adhesive system of *Stenus* beetles achieves much higher adhesive forces with lower applied forces. One might speculate that this is advantageous, since the adhesive secretion of *Stenus* beetles might behave in a non-Newtonian manner (cf. Gorb, 2001; Federle et al., 2002; Vötsch et al., 2002; Drechsler and Federle, 2006; Dirks et al., 2009) and such behaviour in interaction with a relatively low compressive force would improve its flow into surface irregularities. In contrast, higher compressive forces would cause the secretion to behave more solid-like, resulting in pushing away the prey (see supplementary video mmc3 in Appendix A)

Adhesion is affected by the area of contact, which is a function of the normal load, surface roughness and mechanical properties of both contacting materials (Bhushan, 2003). During the predatory strike of the beetles, a substantial impact (compressive) force is attained, because the distance to the prey that must be bridged by the labium only amounts to half the length of the labium (Betz, 1996, 1998). Additionally, the beetles often perform forward lunges during the strike (Betz, 1996, 1998). The resulting increased compressive force (Table 1) should help to further enhance adhesion
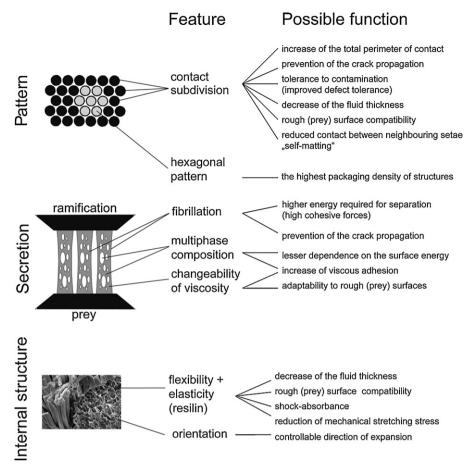
Fig. 9. Summary of the observed structural principles (regarding pattern, secretion and internal structure) and the possibly resulting functional features in the sticky pads of *Stenus* beetles.

by reducing the thickness of the secretion layer (Bowden and Tabor, 1986) and by pressing both the adhesive contacts and the secretion into the irregularities of the prey surface. In tarsal adhesive systems, the adhesion force has been shown to increase with increasing applied normal force and to remain constant when the applied force exceeds a certain value (Jiao et al., 2000; Scherge and Gorb, 2001). Betz (1996) assumed that the push (compressive force) that contacts the prey should be as large as possible in order to achieve considerable adhesive forces. Accordingly, compressive and adhesive forces might be expected to be positively correlated. In contrast to this assumption, in most investigated individuals of both species no such correlation has been observed. However, since the intraspecific variation of the compressive force is very low (Table 1), a relationship between the compressive and the adhesive forces is difficult to detect within a species. Only a broader interspecific comparison might reveal a relation between both of these forces.

A possible insight into the influence of the compressive force on the adhesive performance may be gained from a comparison of the two *Stenus* species. The investigated *S. juno* beetles have significantly smaller pad areas than *S. bimaculatus* (Table 2) but seem to compensate for this disadvantage by generating higher compressive forces, so that the beetles of both species achieve almost identical adhesive properties (Table 1). Interestingly, whereas the prey-capture success of both species is equal for large springtails (Table 3), *S. juno* beetles with their smaller sticky pads attain even higher prey-capture success rates when catching springtails of small body size (Table 3; Betz, 1998). Variations of the attack distance may account for this enhanced compressive force in *S. juno*. Betz (1996, 1998) points out that the difference

between the "critical attack distance" and the length of the forward body lunge performed by the beetles during the strike is equivalent to the attack distance to the prey that must be bridged by the labium. Since the *Stenus* labium is approximately twice as long as the remaining distances to be bridged, it is able to transfer a significant compressive force to the prey (Betz, 1996). Hence, the ability to vary this critical attack distance might be a powerful technique to adjust the strength of the catapult mechanism to the demands. Indeed, towards small springtails, *S. juno* beetles attain significantly smaller attack distances than *S. bimaculatus* (Betz, 1998). Alternatively, one may speculate whether the beetles are capable of adjusting the amount of the haemolymph pressure that is used for the catapult-like protrusion of the labium.

The tenacity (adhesive strength) generated by insect locomotory organs, measured perpendicularly to the contact surface, lies between 2 kPa (*T. viridissima*; Jiao et al., 2000) and 80 kPa (*H. cyanea*; Attygalle et al., 2000). The tenacities of the adhesive systems investigated in the present study (*S. bimaculatus*: 50 kPa; *S. juno*: 70 kPa) correspond well to this range. Higher lateral tenacity (shear strength) has been found in the locomotory organs of insects when measured parallel to the contact surface so that friction forces become more strongly involved (e.g., *Calliphora vomitoria* L., Diptera, Calliphoridae: 280 kPa; Walker, 1993).

4.3. Mechanism of adhesion

Previous investigations (Kölsch and Betz, 1998; Kölsch, 2000; Betz and Kölsch, 2004) have proposed the mode of adhesion in the labial sticky pads of *Stenus* beetles to be in accordance with the principle of Stefan adhesion, in which the viscosity of the secretion

plays the major role. Adhesion based on the formation of covalent bonds or on a type of glue that has to dry was ruled out, because of the high speed of the predatory strike (Kölsch, 2000). Also, the presence of an adhesive secretion makes dry adhesion attributable to van der Waals forces unlikely (Kölsch, 2000; Betz and Kölsch, 2004).

Kölsch (2000) calculated the strongest adhesive force attributable to Stefan adhesion to be 6.64×10^{-5} N in the species *S. comma*. Our results reveal that the measured adhesive forces are more than two orders of magnitude above these calculations (*S. juno*: 1.0×10^{-3} N; *S. bimaculatus*: 1.1×10^{-3} N). These measurements agree well with our theoretically determined adhesive force attributable to Stefan adhesion, which amounts to 0.98×10^{-3} N in *S. juno* and 2.21×10^{-3} N in *S. bimaculatus*. The theoretically calculated adhesive forces attributable to the surface tension of the secretion (see above) amounted to 7.49×10^{-5} N in *S. juno* and 9.17×10^{-5} N in *S. bimaculatus*. Therefore, adhesion is unlikely to be exclusively attributable to the surface tension. Moreover, the large amount of secretion involved (cf. Kölsch, 2000) argues against this mechanism playing a major role. These estimations make it plausible that Stefan adhesion is the major mechanism involved in the investigated adhesive system.

According to formula (1), Stefan adhesion is influenced by various parameters; thus there are different ways of optimizing the efficiency of the prey-capture apparatus (Betz, 1996; Kölsch, 2000). In order to improve the adhesive performance, the effective contact area should be high, whereas the thickness of the secretion layer (distance to the prey) should be low. The final thickness at the moment of contact with the prey presumably depends on the impact force during the predatory strike of the beetle. Thus, the significantly higher compressive forces generated by *S. juno* as compared to *S. bimaculatus* should reduce the thickness of the secretion layer in the contact area. This might be responsible for the observed enhanced adhesion in this species. Additionally, a highly viscous secretion is advantageous for adhesion. Kölsch (2000) estimated the viscosity of the secretion to lie between the viscosities of water (0.001 N s m^{-2}) and plant oils (0.01 N s m^{-2}). Indeed, our calculations reveal viscosities of 0.005 N s m^{-2} for *S. bimaculatus* and 0.01 N s m^{-2} for *S. juno* (calculated according to formula (1)), although the multiphasic chemical composition might further complicate these conditions by changing viscosity depending on the shear rate of the fluid (e.g., Dirks et al., 2009). Finally, the adhesive force resulting from Stefan adhesion can be increased by rapid retraction of the labium after prey capture (Kölsch, 2000; Betz and Kölsch, 2004) in order to bring the prey into the range of the mandibles.

4.4. Safety factor

Prey animals have developed diverse strategies to evade the hunting strategies of their predators (see review by Betz and Kölsch, 2004). For instance, springtails possess a powerful mechanism to escape from the adhesive surface of the predator (e.g., Christian, 1979). According to Kölsch (2000), the tractive force required (F_{requ}) for pulling the prey towards the predator is 0.0203 μN for small (body mass 8.4 μg) and 0.159 μN for large (body mass 62.3 μg) collembolans. According to our force measurements, *S. juno* and *S. bimaculatus* beetles generate adhesive forces (F_a) of ca. 1.0×10^3 μN, corresponding to 6289 times (large springtails) and 49261 times (small springtails) the required forces. These safety factors ($SF = F_a/F_{requ}$) seem to be so large that the prey-capture success particularly towards large springtails should theoretically be much higher than that observed. However, these springtails are able to escape from the adhesive surface of the predator by releasing their powerful escape jump. In this way, they achieve maximum accelerations of 1000 m s^{-2} (Christian, 1979). Consequently, small

and large collembolans produce forces (F_{Coll}) of 8.4×10^{-6} N and 6.23×10^{-5} N, respectively (as calculated by using the formula force = mass × acceleration). According to these calculations, the investigated *Stenus* species achieve safety factors ($SF = F_a/F_{Coll}$) of about 16 (large springtails) to 120 (small springtails). Therefore, the adhesive forces generated by *Stenus* beetles are theoretically sufficient to withstand a possible escape jump of a collembolan. However, a further reduction of the real safety factors is likely, because the prey items possess a variety of surface structures (setae, scales, waxy layers) that might easily get detached from their body surfaces when the beetle tries to retract the prey-capture device (Bauer and Pfeiffer, 1991; Betz and Kölsch, 2004). Additionally, these structures might contaminate the sticky pads, thus reducing the contact area between the labial prey-capture apparatus and the springtail surface in future prey-capture events.

4.5. Presence and function of resilin

According to Betz (1996) the adhesive outgrowths of *Stenus* beetles are strongly elastic. SEM photographs taken after the strike reveal no bending of the setae, although the sticky cushions are significantly compressed. This functional feature is due to the sticky pads being composed of a flexible, highly elastic cuticle containing resilin, an elastic protein (cf. Fig. 8). Resilin enables reversible deformation with extremely high resilience and provides low stiffness, high strain and efficient elastic energy storage (low elastic modulus) (Weis-Fogh, 1960; Andersen and Weis-Fogh, 1964; Gosline et al., 2002).

In the labial adhesive system of *Stenus* species, similar to insect tarsal adhesive systems (Niederegger and Gorb, 2003; Perez Goodwyn et al., 2006), resilin presumably makes the sticky pads flexible, resilient and, therefore, adaptable to the shape and surface irregularities of the prey. Since the labium is used for prey capture several hundred times during the beetle's life, resilin also makes the pads resistant to material fatigue, similar to the function of resilin in insect wing folds (Haas et al., 2000a,b). These possible material attributes are supported by our high-speed video recordings, which show that sticky pads and their outgrowths are able to deform extensively in both directions (i.e., compression and tension) and to regain their initial shape (Fig. 6, frames 7–13). In addition, the material of the sticky pads consists of a reticulum of endocuticular fibres, which further contribute to their flexibility and mechanical stability (Betz, 1996; Kölsch and Betz, 1998; Betz and Kölsch, 2004). Compression of the reticulum provides further adjustment to the outer shape of the prey (Kölsch and Betz, 1998).

4.6. Adhesive secretion

Possible functions of the adhesive secretion are summarised in Fig. 9 (see Betz, 2010 for a general review of the chemical and functional properties of insect adhesive secretion). The secretion released into the contact zone between the sticky pad and the potential prey (as is the case in the tarsi of many insects) is essential for the functioning of this adhesive system. However, the amount of secretion in *Stenus* beetles is considerably higher than in insect tarsi (Figs. 2C and 6; Kölsch, 2000). The main function of the adhesive secretion in the investigated prey-capture apparatus seems to be to increase the actual contact with rough prey surfaces. The compensation for surface roughness is generally considered to be of major importance in wet adhesive systems (Kendall, 2001; Drechsler and Federle, 2006; Persson, 2007; Gorb, 2008). In *Stenus* beetles, the secretion also has to compensate for diverse surface structures that have the potential to reduce prey-capture success (Bauer and Pfeiffer, 1991; Betz and Kölsch, 2004).

Furthermore, we can assume that the viscosity of the secretion rapidly changes during the prey-capture process. It is highly liquid when it is transported from special glands (described in Kölsch, 2000) within the head capsule to the sticky pads. Direct observations of the secretion suggest that it becomes more viscous upon contact with the (prey) surface (Fig. 7 B). The factors responsible for this increase in viscosity are unclear. One assumption is that the adhesive components are dissolved in a low-viscosity liquid that facilitates the transport of the secretion towards the sticky pads. Upon contact with the air, the solvent will evaporate, resulting in the observed increase in viscosity. Since the predatory system of *Stenus* beetles works at high speed, however, such a process is unlikely (Kölsch, 2000).

Another explanation might be that the biphasic adhesive secretion of *Stenus* beetles behaves in a non-Newtonian manner, showing shear-thickening depending on the shear rate of the fluid during the retraction of the labium (see above). A possible advantage of such emulsion-like colloids consisting of both hydrophilic and hydrophobic compounds would be their effective spreading over surfaces of various surface energies (Kölsch, 2000; Gorb, 2001; Vötsch et al., 2002).

The high viscosity of the secretion has been confirmed by our high-speed video recordings of the sticky pads during retraction from a surface (see supplementary video mmc2 in Appendix A). Similar to the behaviour of pressure-sensitive adhesives (e.g., Creton, 2003), the secretion stretches and splits into long fibres before it finally tears off at the contact zone with the substratum (Fig. 6, frames 9–14). This is indicative of the high viscosity of the adhesive imparting a high cohesive strength. Other possible advantages discussed in the context of adhesive fibrillation are the prevention of crack propagation (Ghatak et al., 2004; Chung and Chaudhury, 2005) and the fact that larger amounts of energy are required for the separation of multiple filaments due to higher energy dissipation (Creton, 2003).

5. Conclusions

The investigated adhesive system combines typical functional features of both wet and dry adhesive systems (Fig. 9). The existence of hierarchically structured sticky pads and the high density and small dimensions of the ramifications are comparable with the dry adhesive systems of geckos, anoles, and spiders. However, in the system of *Stenus* species, an adhesive secretion is present, which makes this system similar to the wet adhesive systems of insects, although in contrast to these systems, the adhesive outgrowths of *Stenus* mouthparts are deeply immersed within the secretion and only the tips of their terminal ramifications protrude.

Our *in vivo* force measurements revealed much lower values for the compressive force than for the resulting adhesive force. Although both investigated species differ significantly in their pad morphology (e.g., the pad area and the density of adhesive outgrowths and ramifications), they develop almost identical adhesive forces during predation. A possible explanation for this fact is the generation of higher compressive forces in *S. juno*, the species with a smaller pad area.

Force measurements and high-speed video recordings support the view that viscous forces (Stefan adhesion) are the major adhesive principle involved in the investigated adhesive system. Our measurements agree well with the theoretically estimated adhesive force attributable to Stefan adhesion.

The sticky pads have been modified in various ways during the course of *Stenus* evolution (Betz, 1996, 1998; Puthz, 1998, 2005). Thus, we can conclude that the pad morphology influences adhesion and directly affects prey-capture success. To test the role of the various pad morphologies and impact forces on adhesive performance, a broader range of *Stenus* species should be tested.

Acknowledgments

Appendix A. Supplementary data

Supplementary data associated with this article can be found, in the online version, at doi:10.1016/j.zool.2011.09.006.

References

Alexander, R.M., 1992. Exploring Biomechanics: Animals in Motion. Scientific American Library, New York.

Andersen, S.O., Weis-Fogh, T., 1964. Resilin. A rubberlike protein in arthropod cuticle. Adv. Insect Physiol. 2, 1–65.

Attygalle, A.B., Aneshansley, D.J., Meinwald, J., Eisner, T., 2000. Defense by foot adhesion in a chrysomelid beetle (*Hemisphaerota cyanea*): characterization of the adhesive oil. Zoology 103, 1–6.

Autumn, K., Sitti, M., Liang, Y.A., Peattie, A.M., Hansen, W.R., Sponberg, S., Kenny, T.W., Fearing, R., Israelachvili, J.N., Full, R.J., 2002. Evidence for van der Waals adhesion in gecko setae. Proc. Natl. Acad. Sci. U.S.A. 99, 12252–12256.

Bauer, T., Pfeiffer, M., 1991. 'Shooting' springtails with a sticky rod: the flexible hunting behaviour of *Stenus comma* (Coleoptera, Staphylinidae) and the counter-strategies of its prey. Anim. Behav. 41, 819–828.

Betz, O., 1996. Function and evolution of the adhesion-capture apparatus of *Stenus* species (Coleoptera, Staphylinidae). Zoomorphology 116, 15–34.

Betz, O., 1998. Comparative studies on the predatory behaviour of *Stenus* spp. (Coleoptera: Staphylinidae): the significance of its specialized labial apparatus. J. Zool. Lond. 244, 527–544.

Betz, O., 1999. A behavioural inventory of adult *Stenus* species (Coleoptera: Staphylinidae). J. Nat. Hist. 33, 1691–1712.

Betz, O., 2006. Der Anpassungswert morphologischer Strukturen: Integration von Form, Funktion und Ökologie am Beispiel der Kurzflügelkäfer-Gattung *Stenus* (Coleoptera, Staphylinidae). Entomol. heute 18, 3–26.

Betz, O., 2010. Adhesive exocrine glands in insects: morphology, ultrastructure, and adhesive secretion. In: Byern, J., Grunwald, I. (Eds.), Biological Adhesive Systems. From Nature to Technical and Medical Application. Springer, Berlin, pp. 111–152.

Betz, O., Kölsch, G., 2004. The role of adhesion in prey capture and predator defence in arthropods. Arthr. Str. Dev. 33, 3–30.

Betz, O., Koerner, L., Gorb, S.N., 2009. An insect's tongue as the model for two-phase viscous adhesives? Adhesion 3, 32–35.

Bhushan, B., 2003. Adhesion and stiction: mechanisms, measurement techniques, and methods for reduction. J. Vac. Sci. Technol. B 21, 2262–2296.

Bowden, F.P., Tabor, D., 1950. The Friction and Lubrication of Solids. Oxford University Press, Oxford (reprint 1986).

Chan, E.P., Greiner, C., Arzt, E., Crosby, A.J., 2007. Designing model systems for enhanced adhesion. MRS Bull. 32, 496–503.

Christian, E., 1979. Der Sprung der Collembolen. Zool. Jb. Physiol. 83, 457–490.

Chung, J.Y., Chaudhury, M.K., 2005. Roles of discontinuities in bio-inspired adhesive pads. J. R. Soc. Interface 2, 55–61.

Creton, C., 2003. Pressure-sensitive adhesives: an introductory course. MRS Bull. 28, 434–439.

Dirks, J.-H., Clemente, C.J., Federle, W., 2009. Insect tricks: two-phasic foot pad secretion prevents slipping. J. R. Soc. Interface 7, 587–593.

Drechsler, P., Federle, W., 2006. Biomechanics of smooth adhesive pads in insects: influence of tarsal secretion on attachment performance. J. Comp. Physiol. A 192, 1213–1222.

Federle, W., 2006. Why are so many adhesive pads hairy? J. Exp. Biol. 209, 2611–2621.

Federle, W., Riehle, M., Curtis, A.S.G., Full, R.J., 2002. An integrative study of insect adhesion: mechanics and wet adhesion of pretarsal pads in ants. Integr. Comp. Biol. 42, 1100–1106.

Ghatak, A., Mahadevan, L., Chung, J.Y., Chaudhury, M.K., Shenoy, V., 2004. Peeling from a biomimetically patterned thin elastic film. Proc. R. Soc. Lond. A 460, 2725–2735.

Gorb, S.N., 1999. Serial elastic elements in the damselfly wing: mobile vein joints contain resilin. Naturwissenschaften 86, 552–555.

Gorb, S.N., 2001. Attachment Devices of Insect Cuticle. Kluwer Academic Publishers, Dordrecht.

Gorb, S.N., 2004. The jumping mechanism of cicada Cercopis vulnerata (Auchenorrhyncha, Cercopidae): skeleton–muscle organisation, frictional surfaces, and inverse-kinematic model of leg movements. Arthr. Str. Dev. 33, 201–220.

Gorb, S.N., 2008. Smooth attachment devices in insects. In: Casas, J., Simpson, S.J. (Eds.), Advances in Insect Physiology, vol. 34: Insect Mechanics and Control. Elsevier, London.

Gosline, J.M., Lillie, M., Carrington, E., Guerette, P., Ortlepp, C., Savage, K., 2002. Elastic proteins: biological roles and mechanical properties. Phil. Trans. R. Soc. B 357, 121–132.

Haas, F., Gorb, S.N., Wootton, R.J., 2000a. Elastic joints in dermapteran hind wings: materials and wing folding. Arthr. Str. Dev. 29, 137–146.

Haas, F., Gorb, S.N., Blickhan, R., 2000b. The function of resilin in beetle wings. Proc. R. Soc. Lond. B 267, 1375–1381.

Huber, G., Mantz, H., Spolenak, R., Mecke, K., Jacobs, K., Gorb, S.N., Arzt, E., 2005. Evidence for capillarity contributions to gecko adhesion from single spatula nanomechanical measurements. Proc. Natl. Acad. Sci. U.S.A. 102, 16293–16296.

Israelachvili, J.N., 1991. Intermolecular and Surface Forces. Academic Press, London.

Jagota, A., Benninson, S.J., 2002. Mechanics of adhesion through a fibrillar microstructure. Integr. Comp. Biol. 42, 1140–1145.

Jiao, Y., Gorb, S.N., Scherge, M., 2000. Adhesion measured on the attachment pads of Tettigonia viridissima (Orthoptera, Insecta). J. Exp. Biol. 203, 1887–1895.

Kendall, K., 2001. Molecular Adhesion and Its Applications. Kluwer Academic Publishers, New York.

Koerner, L., Gorb, S.N., Betz, O., 2012. Adhesive performance of the stick-capture apparatus of rove beetles of the genus Stenus (Coleoptera, Staphylinidae) toward various surfaces. J. Insect Physiol. 58, 155–163.

Kölsch, G., 2000. The ultrastructure of glands and the production and function of the secretion in the adhesive capture apparatus of Stenus species (Coleoptera: Staphylinidae). Can. J. Zool. 78, 465–475.

Kölsch, G., Betz, O., 1998. Ultrastructure and function of the adhesion-capture apparatus of Stenus species (Coleoptera: Staphylinidae). Zoomorphology 118, 263–272.

Langer, M.G., Ruppersberg, J.P., Gorb, S.N., 2004. Adhesion forces measured at the level of a terminal plate of the fly's seta. Proc. R. Soc. Lond. B 271, 2209–2215.

Mate, C.M., 2008. Tribology on the Small Scale: A Bottom up Approach to Friction, Lubrication, and Wear. Oxford University Press, Oxford.

McFarlane, J.S., Tabor, D., 1950. Adhesion of solids and the effect of surface films. Proc. R. Soc. Lond. A 202, 224–243.

Niederegger, S., Gorb, S.N., 2003. Tarsal movements in flies during leg attachment and detachment on a smooth substrate. J. Insect Physiol. 49, 611–620.

Owens, D.K., Wendt, R.C., 1969. Estimation of the surface free energy of polymers. J. Appl. Polym. Sci. 13, 1741–1747.

Peressadko, A., Gorb, S.N., 2004. Surface profile and friction force generated by insects. In: Boblan, I., Bannasch, R. (Eds.), Fortschritt-Berichte VDI, vol. 249. VDI Verlag, Düsseldorf, pp. 257–263.

Perez Goodwyn, P., Peressadko, A., Schwarz, H., Kastner, V., Gorb, S.N., 2006. Material structure, stiffness, and adhesion: why attachment pads of the grasshopper (Tettigonia viridissima) adhere more strongly than those of the locust (Locusta migratoria) (Insecta: Orthoptera). J. Comp. Physiol. A 192, 1233–1243.

Persson, B.N.J., 2007. Biological adhesion for locomotion on rough surfaces: basic principles and a theorist's view. MRS Bull. 32, 486–490.

Puthz, V., 1998. Die Gattung Stenus Latreille in Vietnam (Coleoptera, Staphylinidae). Rev. Suisse Zool. 105, 383–394.

Puthz, V., 2005. Neue und alte neotropische Stenus (Hemistenus-) Arten (Coleoptera: Staphylinidae). Mitteilungen Int. Entomol. Vereins Suppl. XI, 1–60.

Puthz, V., 2010. Stenus Latreille, 1797 aus dem Baltischen Bernstein nebst Bemerkungen über andere fossile Stenus-Arten (Coleoptera, Staphylinidae). Ent. Bl. 106, 265–287.

Rohlf, F.J., 2004. tpsDig, Version 2.0. Department of Ecology and Evolution, State University of New York at Stony Brook.

Scherge, M., Gorb, S.N., 2001. Biological Micro- and Nanotribology. Springer, Berlin.

Schmitz, G., 1943. Le labium et les structures bucco-pharyngiennes du genre Stenus Latreille. Cellule 49, 291–334.

Spolenak, R., Gorb, S.N., Arzt, E., 2005a. Adhesion design maps for bioinspired attachment systems. Acta Biomater. 1, 5–13.

Spolenak, R., Gorb, S.N., Gao, H., Arzt, E., 2005b. Effect of contact shape on the scaling of biological attachments. Proc. R. Soc. Lond. A 461, 305–319.

Stork, N.E., 1980. Experimental analysis of adhesion of Chrysolina polita (Chrysomelidae: Coleoptera) on a variety of surfaces. J. Exp. Biol. 88, 91–107.

Varenberg, M., Peressadko, A., Gorb, S.N., Arzt, E., 2006. Effect of real contact geometry on adhesion. Appl. Phys. Lett. 89, 121905.

Varenberg, M., Pugno, N., Gorb, S.N., 2010. Spatulate structures in biological fibrillar adhesion. Soft Matter 6, 3269–3272.

Voigt, D., Schuppert, J.M., Dattinger, S., Gorb, S.N., 2008. Sexual dimorphism in the attachment ability of the Colorado potato beetle Leptinotarsa decemlineata (Coleoptera: Chrysomelidae) to rough substrates. J. Insect Physiol. 54, 765–776.

Vötsch, W., Nicholson, G., Müller, R., Stierhof, Y.-D., Gorb, S.N., Schwarz, U., 2002. Chemical composition of the attachment pad secretion of the locust Locusta migratoria. Insect Biochem. Mol. Biol. 32, 1605–1613.

Walker, G., 1993. Adhesion to smooth surfaces by insects – a review. Int. J. Adhes. 13, 3–7.

Weinreich, E., 1968. Über den Klebfangapparat der Imagines von Stenus Latr. (Coleopt., Staphylinidae) mit einem Beitrag zur Kenntnis der Jugendstadien dieser Gattung. Z. Morph. Ökol. Tiere 62, 162–210.

Weis-Fogh, T., 1960. A rubber-like protein in insect cuticle. J. Exp. Biol. 37, 887–907.